

Parameters Assessment for Industrial 5G Networks

¹Christian Mailer, ¹Alex Sandro Roschildt Pinto and ²Adao Boava

¹Department of Informatics and Statistics, Federal University of Santa Catarina, Brazil

²Department of Control Engineering and Automation, Federal University of Santa Catarina, Brazil

Article history

Received: 06-05-2022

Revised: 10-07-2022

Accepted: 14-07-2022

Corresponding Author:

Christian Mailer

Department of Informatics and Statistics, Federal University of Santa Catarina, Brazil

Email: c.mailer@posgrad.ufsc.br

Abstract: The Fifth Generation of Mobile Networks (5G) will allow low latency to be achieved while providing high reliability. This service grade will suit industrial applications very well since it will allow the integration of a wireless framework without compromising the determinism of industrial networks. Employing Time-Sensitive Networking (TSN) standards in the 5G architecture is currently the best solution to maintain compatibility with existing industrial implementations and to make the mobile network capable of providing the required synchronization and low latency. However, there is not much research that explores the quantitative elements behind 5G architectures applied to industry, which would be essential for designing and managing mobile TSN networks. This study explored the influence of numerology and payload size on 5G networks through simulations and graphical analysis. The results showed that for frequencies below 6 GHz, numerology 4 should be used. For a frequency of 26 GHz, numerology 3 and 4 are acceptable, but 4 proved to be more suitable for critical applications. For packet sizes above 650 bytes, it was concluded that the 26 GHz frequency should be used.

Keywords: 5G, Industry 4.0, URLLC, TSN, Numerology, Latency, Simulation

Introduction

Ultra-Reliable Low Latency Communication (URLLC) is one of the service grades served by the Fifth Generation of Mobile Networks (5G) and it is intended for applications that require latency up to 1 ms. This feature is essential for the industry, offering a mobile reliable, and robust model that allows exploring resources covered by the industry 4.0 concept.

Among the benefits of using a wireless architecture in the industry is Flexibility in the connection between devices, reduced installation and maintenance costs, mobility, and less human exposure to risk situations (Aijaz, 2020). Furthermore, when using 5G as an industrial communication technology, there are even more benefits that are not found in the technologies that existed before it, such as Quality of Service (QoS) for critical applications; support for high transfer rates, and a large number of devices; security; built-in support for mobility; better accuracy for tasks that require positioning (Aijaz, 2020).

A key point for supporting industrial applications is the integration of 5G with Time-Sensitive Networking (TSN) resources. TSN is a standard, defined by the IEEE 802.1 Working Group, which allows for configuring a deterministic and reliable low latency

communication. 3GPP Release 16 standardizes a model for integrating TSN into a centrally managed 5G network using a TSN Bridge architecture.

Two other architectures that can be adopted to integrate TSN into 5G networks are TSN Link and Integrated TSN Framework (Striffler *et al.*, 2019). However, such models were not standardized by 3GPP and, despite having great advantages, would require more effort and time for standardization and implementation.

Considering that the TSN architectures in the 5G network are already mapped and even a model is standardized by 3GPP, it is now necessary to carry out research aimed at estimating delays, efficiency, equations, and other empirical data that may be useful for the design of a 5G-based industrial network. With this, it is possible to foresee the constraints and the best equipment or industrial protocols (e.g., PROFINET, EtherCAT, IRT, Sercos III, etc.) to be used in a real environment.

Few studies perform a performance evaluation of industrial 5G network models in terms of protocols, configuration, interference, and bottlenecks.

Developing studies on the topic is not only relevant for regulations, but also for optimizing the design and planning of an industrial wireless infrastructure based on 5G.

By having analytical results, it is possible to indicate which are the best choices of protocols or standards for each case and even make it possible to study new architectures not yet conceived.

In addition to the points listed above, it is also necessary to map the possible simulation tools, as well as their functionalities, which can help in the modeling and evaluation of mathematical models. Simulators should be an effective and less expensive alternative than a physical environment, making testing with multiple UEs (User Equipment) and different architectures easier and reducing manual effort, since the scenario can be defined and changed virtually and automatically.

The probabilistic modeling of access, Core, and network behavior are also valuable information, since they demonstrate the variation of some parameters as a function of another specific parameter, serving as a reference for 5G systems to adapt dynamically, according to the environment and traffic. However, such models are rare and there are no studies that estimate them for an industrial application.

This study proposes the simulation of a 5G architecture applied to industry and estimates the influence of numerology and payload size on jitter and latency, obtaining a mathematical model of delay in the function of payload size for numerologies 3 and 4.

In the Related Works section, other researches involving 5G for the industry are described along with the differences between them and the present work. In the Methodology section, the simulation environment and the configured parameters are detailed. The results were analyzed and a mathematical model was obtained in the Results section. Final considerations, the contribution of experiments for the academic society, and future works were written in the Conclusions section.

Larrañaga *et al.* (2020) surveyed the current progress involving the integration of TSN to 5G networks. After describing all the concepts and important characteristics of the theme, the authors considered an industrial scenario and raised some points to be explored, such as the delay in the TSN-5G bridge. The calculations of the parameters involved were thoroughly described and, in the end, the authors concluded that the implementation of an optimized local 5G Core is essential to achieve a viable delay and that, to support the periodic traffic, semipersistent scheduling in Down Link (DL) or a configured schedule with periodic resources must be used. The work did not perform any type of simulation and did not address factors related to the environment (e.g., distance and interference).

Khoshnevisan *et al.* (2019) described the requirements, which include frequency, architecture, and protocol, for the

URLLC service grade in a 5G network for an industrial environment. As a solution to possible radio interference that, according to the authors, can occur in an application in the industry, the use of the Coordinated Multipoint (CoMP) transmission method is proposed, which would not require packet retransmission. Several CoMP techniques are tested through simulations to obtain a graphical analysis of their advantages. Furthermore, the authors analyze more characteristics of the integration of a TSN network to 5G, such as the percentage gain of the compression of Ethernet headers, encapsulation procedure of an Ethernet PDU (Protocol Data Unit) in a 5G network and proposals for solutions to synchronization errors in communication. Finally, a prototype was assembled with motors, a Programmable Logic Controller (PLC), and a 5G radio emulator for latency analysis when using the PROFINET RT protocol. The simulation was performed taking into account frequency factors and numerical delay data were collected, proving the effectiveness of the experiment. Future work includes improving achieved latencies and testing in real industrial environments. The experiment considered only one central frequency (3 GHz) and one band (100 MHz) and did not evaluate the performance variation as a function of packet size and numerology. Also, the focus of the evaluation was the CoMP model.

Martenvormfelde *et al.* (2020) developed an open-source model for TSN simulations in 5G networks based on the OMNeT++ software and the NeSTiNg library (for TSN). Several other existing tools were cited, but none fit the authors' needs. Also, it was considered to extend the SimuLTE library, however, the option was later discarded because it was more complex. A closed loop control was tested in the developed simulator and delay data were collected by varying parameters such as frame structure (from 5G radio) and subcarrier spacing. The authors concluded that, for real industrial applications, different slot ranges and poor scheduling decisions can significantly influence QoS and increase delay and jitter. In future work, the authors intend to refine the model and improve compatibility with 3GPP standards. The article did not take into account environmental factors such as distance between devices, height, and interference. Jitter measurements were not presented and the impact of packet size on latency was not evaluated either.

Ginthör *et al.* (2019) described in detail the characteristics required for an industrial network and the relevant factors for integrating TSN into a 5G network. They also propose a simulation model based on the NeSTiNg library and the SimuLTE framework, making the necessary adaptations for 5G. After some tests, the authors created a graph for the traffic pattern, one for the end-to-end latency (worst case) as a function of the number of user devices (UE), one for the throughput as a function of the number of UEs and one of the impacts on latency relative to best effort traffic. Analyzing the

quantitative data, the authors concluded that for industrial requirements, in addition to integrating TSN into 5G networks, end-to-end scheduling is necessary that takes into account factors such as application settings and frame arrival time of the streams involved, points that will be explored by the authors in future works. Frequencies above 6 GHz were not analyzed and the positioning of the UEs and RAN was not taken into account. Jitter values were not displayed and latency variation as a function of packet size and numerology was not considered.

Karamyshev *et al.* (2020) propose two analytical capacity estimation models for URLLC networks, one with high precision and the other with lower computational cost, but with a small margin of error. The authors discuss the step-by-step deduction of the first model (with greater precision), explaining the probabilistic equation used, which is based on the Poisson process. This model is later evaluated through comparisons with simulations in the NS-3 software, proving to be effective for some parameter ranges. Also, using the model obtained, the authors performed some analyzes to measure the influence of system parameters and QoS level on the network capacity. As a way to improve the adaptability of the 5G mobile network to meet URLLC applications, the authors suggested the use of the model in gNB in an online mode, however, for this to be efficiently applicable, an approximate model that requires less computational power was proposed. This model was compared with the first one and the authors reached a maximum error of 12%. According to the article, future works will evaluate scenarios with heterogeneous QoS requirements and the development of efficient admission control algorithms. The authors did not assess latency and jitter variation. The simulation did not use a library that implemented the communication protocols, and the parameters were all based on statistical models.

Materials and Methods

To simulate the environment, the 5G-Lena simulator, offered as a module of the NS-3 software, was used. It is maintained by CCTC (*Centre Tecnològic de Telecomunicacions de Catalunya*), located in Spain, and licensed under GPLv2. Its choice was due to having a more advanced level of development and testing in the radio part, with the PHY (Physical), MAC (Medium Access Control), and RLC (Radio Link Control) layers implemented according to the 3GPP specifications for 5G radio (Patriciello *et al.*, 2019). The upper layers, as well as the Core, are still based on the LTE generation, but they are not essential for the simulations as their functionality is very similar between the LTE and 5G generations.

A simple scenario was defined in the simulator to facilitate the simulation and data collection, thus making it possible to obtain base values. The scenario is composed of access (gNB) and a UE separated by a

horizontal distance of 10 m. The heights of the access and the UE, respectively, are 3 and 1.5 m.

The simulator was configured to assume an Indoor Hotspot-Mixed Office model which, despite not being a model adapted for an industrial case, is the closest to the available options, which include Urban Macrocell and Microcell and Rural Macrocell. This setting is responsible for defining the signal propagation model.

The signal strength for the UE was defined as 4 dBm and for the gNB as 8 dBm since the distance between the devices is not significant and there is no noise in this scenario. The shadowing model was not enabled for the experiments.

5G Quality of Service (5QI) number 80 was used, which is specific for low latency applications. Other more specific levels could also be used for automation, but the simulator similarly treats the levels, so it was preferred to reduce the need for several configurations and use a mode that would be suitable for all the simulations that will be performed.

An ideal Core, with zero latency, was created to serve the UE. It is noteworthy that the experiment aims to evaluate parameters related to the radio and therefore it was chosen to ignore the influence of the interface between gNB and Core and the data network. Figure 1 illustrates the tested architecture.

The stack that will be tested will be the UDP/IP, which, in a real case, could be used to encapsulate Ethernet packets from an industrial network.

The first set of tests aims to evaluate the impact of numerology and frequency on parameters such as delay (end-to-end), jitter, and packet loss corresponding to the transfer of a 100 bytes payload at a transfer rate of 4000 packets per second. For this, numerology from 0 to 4 (15 to 240 kHz) will be tested for frequencies of 26 GHz (200 and 400 MHz bands), 3.5 GHz (40 MHz band), and 2.3 GHz (40 MHz band).

The second set of tests will evaluate the impact of packet size on delay (end-to-end). The payload will vary in length from 50 bytes to 1450 bytes with steps of 100 bytes. The same frequencies of the first set will be tested, however, only numerology 3 (120 kHz) and 4 (240 kHz) will be used.

The simulation time will be 1 s and the tested traffic will be the Downlink one. The simulation results are shown in the Results subsection.

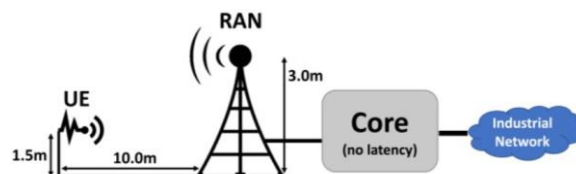


Fig. 1: Simulated architecture

Results and Discussion

The data obtained after the first set of tests were divided into two tables: Table 1, for the average of the latency data, and Table 2, for the average of the jitter data. Data related to packet loss were not displayed in a table as they did not vary, remaining constant at 0%.

As shown in Table 1, it is noted that for latency and jitter, the values obtained at the 2.3 and 3.5 GHz frequencies (both with a 40 MHz band) were the same. For the 26 GHz frequency, there was a small decrease in the latency value and a small increase in the jitter value, however, it is still very close to the 2.3 and 3.5 GHz frequencies, so the variation could be ignored.

The jitter value for numerology 4 in 26 GHz with 200 MHz bandwidth was outside of the expected average. This could be due to some inaccuracy of the simulator.

With Table 1, it is already possible to determine that numerologies below 2 are not viable for applications that demand up to 1 ms of end-to-end latency. Also, it is noteworthy that the exposed latency is an average value, so it does not necessarily indicate that the latency was always below 1 ms.

To better assess the latency distribution, some histograms showing the number of packets exchanged in the simulation interval were plotted. Latency distribution is the same for both bandwidths in 26 GHz and numerology 2 and 3. For numerology 4 and 26 GHz, different distributions were obtained for each bandwidth, which is per the difference in the jitter value found for 26 GHz and 200 MHz bandwidth (refer to Table 2).

Figure 2 and 3 contain the histograms for numerology 2. Figure 4 and 5 contain the histograms for numerology 3. Figure 6, 7, and 8 contain the histograms for numerology 4.

As shown in Fig. 2, a very low number of packets had an end-to-end latency greater than 1 ms. If the application depended on all packets' latency to be below 1 ms, the 2.3 and 3.5 GHz frequencies (40 MHz bandwidth) with numerology 2 cannot be used, but if the application tolerates the delivery of a few packets with a latency above 1 ms, then this configuration would be acceptable. It is noteworthy that the environment can suffer from interference, variation in the number of nodes, and greater distances between the UE and the gNB, which would result in higher latency, therefore, this must be taken into account when choosing numerology and frequency.

In Fig. 3 and 4, some packets had their latency close to 1 ms, which could result in latencies greater than 1 ms in the case of interference or greater distance between UE and gNB. Therefore, numerology 2 with 26 GHz frequency or numerology 3 with 2.3 and 3.5 GHz (40 MHz bands) would not be appropriate if the application depends critically on a latency up to 1 ms, but

numerology 3 could be used at 26 GHz with 200 and 400 MHz bands.

Figures 6, 7, and 8 show that numerology 4 provided delivery of less than 0.7 ms for all packets and, for the case of the 26 GHz frequency and 400 MHz bands, the maximum latency was 0.4 ms. This frequency and band would be more suitable for critical applications.

Figure 9 shows the average end-to-end latency achieved for each tested payload size, as well as the linear or polynomial fit made. These tests correspond to the second part of the experiment.

The linear fit follows the equation $y(x) = Ax + B$, while the polynomial (quadratic) fit follows the equation $y(x) = a_0 + a_1 \cdot x + a_2 \cdot x^2$.

As can be seen in Fig. 9, the frequencies of 2.3 and 3.5 GHz, in numerology 3 and 4, had a polynomial variation in the tested interval. The 26 GHz frequency (200 and 400 MHz bands) showed a linear evolution.

When analyzing only the payload size range between 50 and 550 bytes, it is noted that all frequencies presented very similar values within each tested numerology. The difference in latency, in this interval, between numerology 3 and 4 is approximately 0.2 ms (numerology 4 has lower latency), which can be measured through the analysis of coefficient B. This information demonstrates that the frequency does not impact the average latency for packets of up to 550 bytes, with numerology being the decisive parameter.

In Fig. 9, in the results of numerology 3, the frequency of 26 and the 400 MHz band showed an increase of approximately 158% in the slope compared to the same frequency with the 200 MHz band. In numerology 4, this increase was only 49%, approximately. Although the slope has a small order of magnitude (10^{-5}), it can be said that the latencies in numerology 4 for the 26 GHz frequency in both bands, in the tested payload size range, tend to stay close.

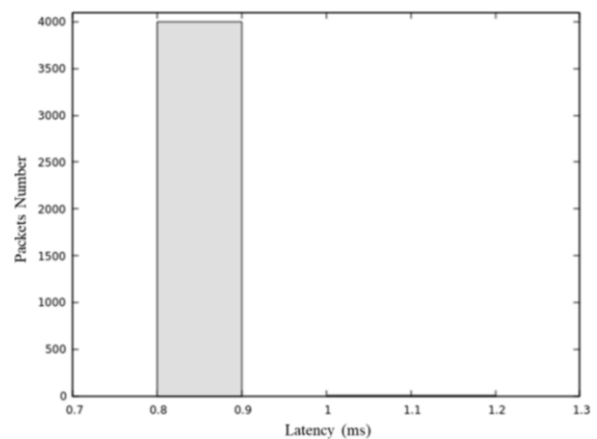


Fig. 2: Latency histogram for numerology 2 and 2.3 GHz and 3.5 GHz frequencies (40 MHz bandwidth)

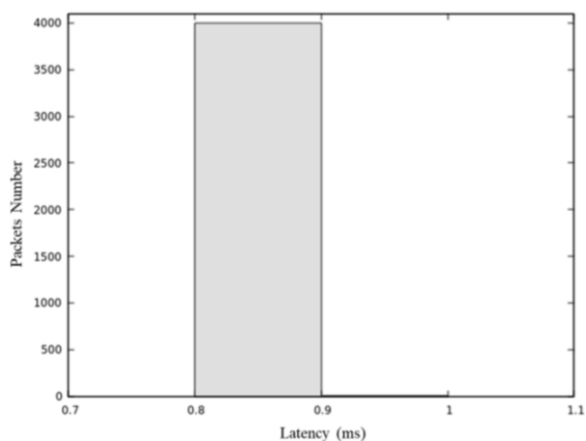


Fig. 3: Latency histogram for numerology 2 and 26 GHz frequency (200 and 400 MHz bandwidths)

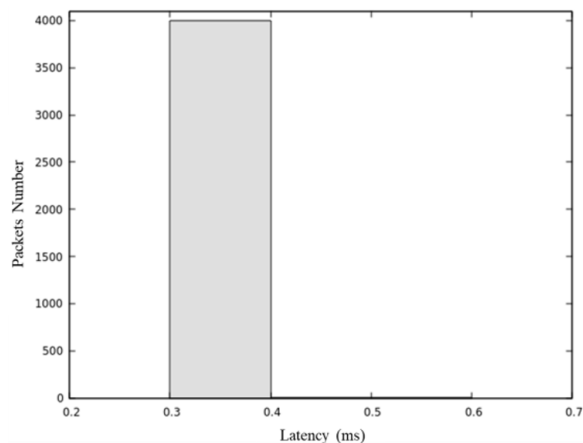


Fig. 6: Latency histogram for numerology 4 and 2.3 GHz and 3.5 GHz frequencies (40 MHz bandwidth)

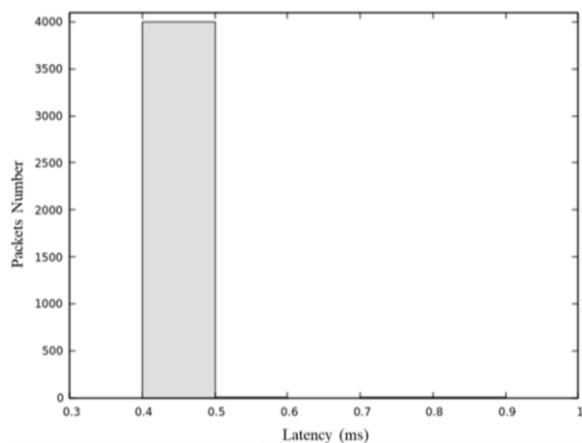


Fig. 4: Latency histogram for numerology 3 and 2.3 GHz and 3.5 GHz frequencies (40 MHz bandwidth)

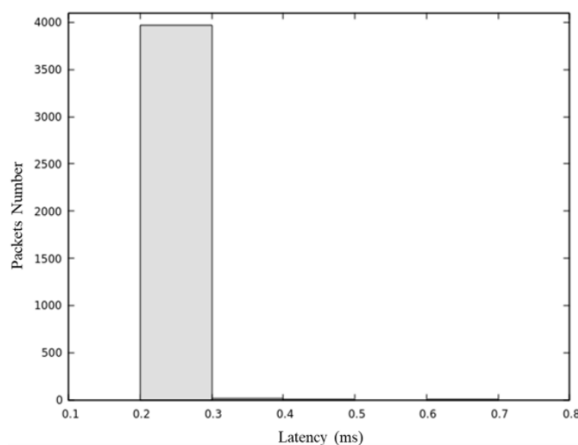


Fig. 7: Latency histogram for numerology 4 and 26 GHz frequency (200 MHz bandwidth)

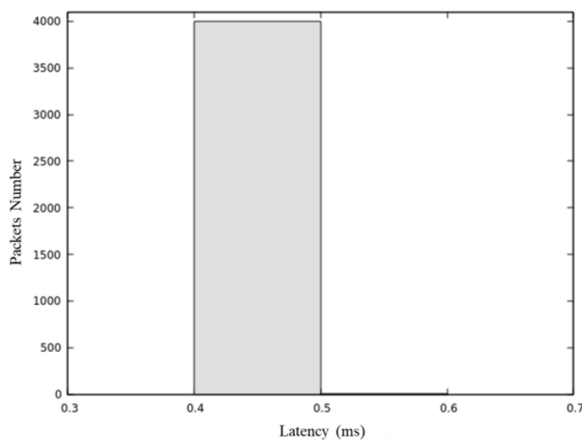


Fig. 5: Latency histogram for numerology 3 and 26 GHz frequency (200 and 400 MHz bandwidths)

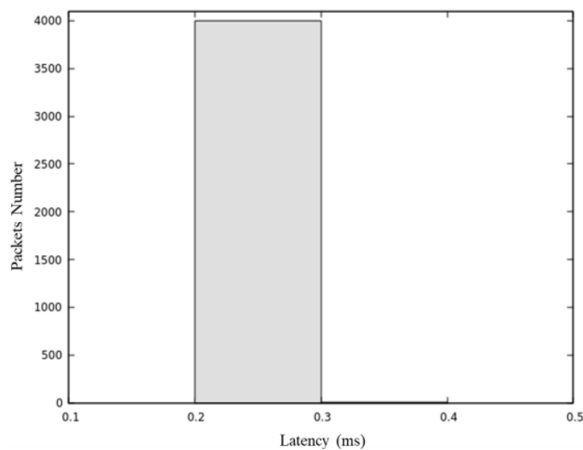


Fig. 8: Latency histogram for numerology 4 and 26 GHz frequency (400 MHz bandwidth)

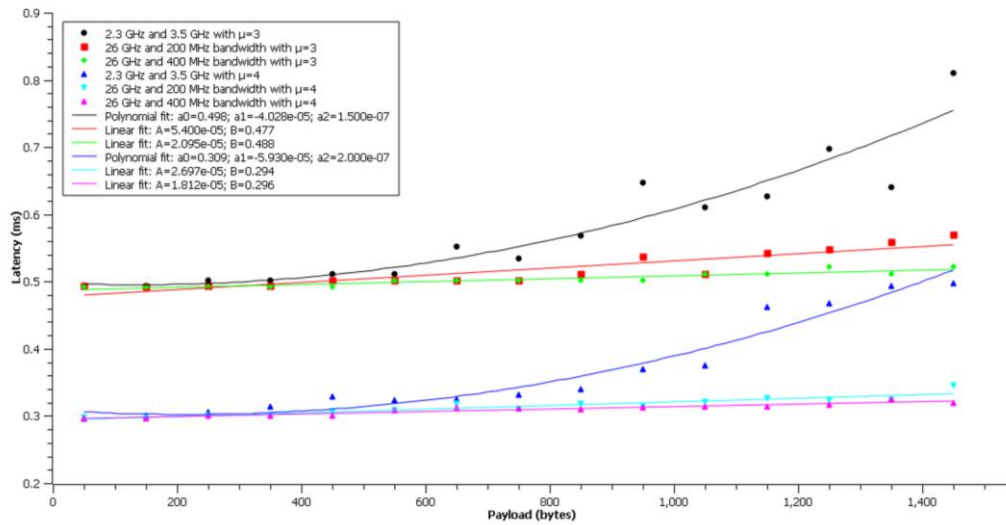


Fig. 9: Average downlink latency as a function of the payload size

Table 1: End-to-end latency values (ms) obtained in each frequency for numerologies μ

Frequency	$\mu=0$	$\mu=1$	$\mu=2$	$\mu=3$	$\mu=4$
26 GHz (400 MHz bandwidth)	2.8683	1.5466	0.8858	0.4929	0.2965
26 GHz (200 MHz bandwidth)	2.8688	1.5467	0.8858	0.4929	0.2976
3.5 GHz (40 MHz bandwidth)	2.8726	1.5477	0.8861	0.4931	0.3010
2.3 GHz (40 MHz bandwidth)	2.8726	1.5477	0.8861	0.4931	0.3010

Table 2: End-to-end jitter values (ms) obtained in each frequency for numerologies μ

Frequency	$\mu=0$	$\mu=1$	$\mu=2$	$\mu=3$	$\mu=4$
26 GHz (400 MHz bandwidth)	0.3748	0.2500	0.0001	0.0001	0.0001
26 GHz (200 MHz bandwidth)	0.3748	0.2500	0.0001	0.0001	0.0017
3.5 GHz (40 MHz bandwidth)	0.3747	0.2499	0.0001	0.0001	0.0001
2.3 GHz (40 MHz bandwidth)	0.3747	0.2499	0.0001	0.0001	0.0001

Conclusion

According to the results, it can be concluded that the numerology parameters and payload size must be correctly adjusted to achieve a latency below 1 ms and that these parameters did not influence packet losses.

Numerologies below 2 were not able to deliver an average latency of up to 1 ms, not being appropriate for industrial scenarios.

In numerology 2, the average latency is within the required limit, however, as it is an average and because it is only 13% away from the maximum limit, this delay might increase on some packets and exceed the limit, a proven fact, in part, by the histogram. Therefore, numerology 2 would not be recommended for industrial networks either.

Numerology 3, on the other hand, presented an average latency of a maximum of 0.5 ms, but at the 2.3 and 3.5 GHz frequencies (40 MHz bands), the histogram showed that some packets arrive very close to the 1 ms limit, which could lead to out-of-bounds deliveries if there is interference, Core delay, TSN-Bridge delay, or distance is increased. This set of

numerology and frequencies (2.3 and 3.5 GHz with 40 MHz bands) would also not be suitable for industrial networks. But for 26 GHz frequency with 200 and 400 MHz bands, this numerology proves to be acceptable.

The numerology that resulted in the lowest latency was 4, which would be the most indicated in critical industrial architecture. In addition, the latency of the 26 GHz frequency with a 400 MHz band is the best one, not presenting any packet with a latency greater than 0.4 ms. Also, it is necessary to emphasize that this average was referring to a payload of 100 bytes.

The impact of payload size on average latency is greater for 2.3 and 3.5 GHz frequencies, presenting quadratic polynomial dynamics. For these sub-6 GHz frequencies, numerology 3 causes latency to rise significantly from 650 bytes up, which contributes to rejecting these sets of frequencies and numerology in industrial networks.

In numerology 4, the average latency of the low frequencies (2.3 and 3.5 GHz) also increases more

significantly from the 650-byte payload up, making this choice of configurations unreliable for critical applications with larger payloads.

For high frequencies, the payload size does not have much influence on the average latency, leading to the conclusion that, for larger packets, the 26 GHz frequency should be used. Also, it is emphasized, again, that numerology 4 would be the most suitable for critical industrial applications since the variation caused in latency was very low.

The data obtained are of great importance for the design of a 5G industrial network, offering performance models for the network elements and the consequences of a given choice of parameters. The experiment provides a reference of what tools are available for this type of simulation and the methods that can be used for related work. In addition, it is possible to list some points that must be developed in the simulator for better accuracy of the results, which are: Path loss and shadowing model for the industrial scenario, adaptation of the upper radio layers to fully meet the 5G NR standardization, 5G Core model (without relying on LTE generation elements) and improvement of 5QI models for better management of critical automation traffic.

Future works can be carried out aiming at analyzing the traffic on the Uplink in isolation and simultaneously with the Downlink. Other protocols can also be tested, such as Ethernet, comparing its efficiency with the UDP/IP stack. Furthermore, the influence of packet throughput rate on latency could be evaluated to analyze the best configuration for the TSN-Bridge, complementing the results found on the payload size. Regarding the scenario, characteristics such as distance and number of UEs and gNBs could be changed to measure the impact on transmission and generate graphs of signal level influence on latency, jitter, and packet loss.

Acknowledgment

The authors would like to thank Stemmer Foundation (FEESC) for partially funding the publication of this article.

Author's Contributions

Christian Mailer: Worked on the literature review, simulations, results in analysis, and conclusion.

Alex Sandro Roschildt Pinto and Adao Boava: Contributed to the results reviewing.

Ethics

The authors certify that the content of this article is original and that it was not previously published. There are no ethical issues involved.

References

- Aijaz, A. (2020). Private 5G: The future of industrial wireless. *IEEE Industrial Electronics Magazine*, 14(4), 136-145. DOI.org/10.1109/MIE.2020.3004975
- Ginhör, D., von Hoyningen-Huene, J., Guillaume, R., & Schotten, H. (2019, November). Analysis of Multi-user Scheduling in a TSN-enabled 5G System for Industrial Applications. In *2019 IEEE International Conference on Industrial Internet (ICII)* (pp. 190-199). IEEE. DOI.org/10.1109/ICII.2019.00044
- Karamyshev, A., Khorov, E., Krasilov, A., & Akyildiz, I. F. (2020). Fast and accurate analytical tools to estimate network capacity for URLLC in 5G systems. *Computer Networks*, 178, 107331. DOI.org/10.1016/j.comnet.2020.107331
- Khoshnevisan, M., Joseph, V., Gupta, P., Meshkati, F., Prakash, R., & Tinnakornsrisuphap, P. (2019). 5G industrial networks with CoMP for URLLC and time-sensitive network architecture. *IEEE Journal on Selected Areas in Communications*, 37(4), 947-959. DOI.org/10.1109/JSAC.2019.2898744
- Larrañaga, A., Lucas-Estañ, M. C., Martinez, I., Val, I., & Gozalvez, J. (2020, September). Analysis of 5G-TSN integration to support industry 4.0. In *2020 25th IEEE International conference on emerging technologies and factory automation (ETFA)* (Vol. 1, pp. 1111-1114). IEEE. DOI.org/10.1109/ETFA46521.2020.9212141
- Martenvormfelde, L., Neumann, A., Wisniewski, L., & Jasperneite, J. (2020, September). A simulation model for integrating 5g into time-sensitive networking as a transparent bridge. In *2020 25th IEEE International Conference on Emerging Technologies and Factory Automation (ETFA)* (Vol. 1, pp. 1103-1106). IEEE. DOI.org/10.1109/ETFA46521.2020.9211877
- Patriciello, N., Lagen, S., Bojovic, B., & Giupponi, L. (2019). An E2E simulator for 5G NR networks. *Simulation Modelling Practice and Theory*, 96, 101933. DOI.org/10.1016/j.simpat.2019.101933
- Striffler, T., Michailow, N., & Bahr, M. (2019, September). Time-sensitive networking in 5th generation cellular networks-current state and open topics. In *2019 IEEE 2nd 5G World Forum (5GWF)* (pp. 547-552). IEEE. DOI.org/10.1109/5GWF.2019.8911720